Clay content and mineralogy, organic carbon and cation exchange capacity affect water vapour sorption hysteresis of soil

Arthur, Emmanuel; Tuller, Markus; Moldrup, Per; de Jonge, Lis W.

Published in:
European Journal of Soil Science

DOI (link to publication from Publisher):
10.1111/ejss.12853

Publication date:
2020

Document Version
Accepted author manuscript, peer reviewed version

Clay content and mineralogy, organic carbon and cation exchange capacity affect water vapour sorption hysteresis of soil

E. ARTHUR[a], M. TULLER[b], P. MOLDRUP[c] & L.W. de JONGE[a]

[a]*Department of Agroecology, Aarhus University, Blichers Allé 20, PO Box 50, DK-8830, Tjele, Denmark*

[b]*Department of Soil, Water, and Environmental Science, The University of Arizona, 1177 E. 4th Street, Tucson, AZ 85721, USA*

[c]*Department of Civil Engineering, Aalborg University, Thomas Manns Vej 23, DK-9220, Aalborg, Denmark*

Correspondence: E. Arthur. Email: emmanuel.arthur@agro.au.dk

Running title: Quantification and controls of sorption hysteresis

This article has been accepted for publication and undergone full peer review but has not been through the copyediting, typesetting, pagination and proofreading process, which may lead to differences between this version and the Version of Record. Please cite this article as doi: 10.1111/ejss.12853

Summary

The hysteretic behaviour of the dry region (< −1.5 MPa) of the soil water characteristic, which is of the essence for accurate characterization and modelling of bio-physicochemical soil processes under dry conditions, is well documented. However, knowledge about how to best quantify water vapour sorption hysteresis and about the effects of soil properties on dry-region hysteretic behaviour is limited. To overcome this knowledge gap, we proposed a new method for quantifying sorption hysteresis and evaluated its applicability based on measured sorption isotherms of four source clay minerals and 147 soil samples. Furthermore, the effects of clay mineralogy, clay content, soil organic carbon (SOC), and cation exchange capacity (CEC) on the magnitude of sorption hysteresis were investigated. For the clay minerals, kaolinite did not exhibit hysteretic behaviour, illite showed some hysteresis, while Na- and Ca-smectite exhibited strong hysteretic behaviour. The average hysteresis, corrected for clay and SOC contents, was strongly reflective of the dominant clay mineralogy of the soil samples. For the soil samples with low SOC content, the average hysteresis significantly increased with increasing clay content (R^2 = 0.92), except for the kaolinite-rich samples (R^2 = 0.35). The SOC-rich samples that exhibited illitic clay mineralogy and similar soil texture showed a significant increase in average hysteresis with increasing organic carbon content (R^2 = 0.93). For all soil samples combined, the CEC was the strongest indicator for the magnitude of water vapour sorption hysteresis.

Keywords: dry region soil water characteristic, soil organic carbon, soil texture, soil particle size distribution, CEC

Highlights

- A new index for quantification of soil vapour sorption hysteresis was proposed
- Large SOC and clay content increased sorption hysteresis
- For soil samples, dominant clay mineralogy controlled the magnitude of hysteresis
- Cation exchange capacity was the best predictor of hysteresis for all soil types

Introduction

Accurate characterization of unsaturated soil behaviour requires an in-depth knowledge of soil water retention dynamics. It is recognized that the soil water characteristic for matric potentials > −1.5 MPa is hysteretic (i.e. at a given matric potential, the water content obtained via wetting is commonly below that retained via drying). To explain this phenomenon, mechanisms such as the ink-bottle effect, differences in advancing and receding liquid-solid contact angles, entrapped air and swelling and shrinking are generally accepted (Tuller & Or, 2005b; Sadeghi *et al.*, 2018). Based on these mechanisms, several models were developed to account for soil water retention hysteresis in the wet region (Kool & Parker, 1987; van Dam *et al.*, 1996; Pedroso & Williams, 2010; Rudiyanto *et al.*, 2015; Zhuang *et al.*, 2017). Nakagawa *et al.* (2012) noted that it is crucial to account for hysteresis in numerical models for unsaturated water flow.

Soil water retention curves in the dry region (< −1.5 MPa), often termed soil water vapour sorption isotherms, are of crucial importance for modelling of volatilization of volatile organic compounds and pesticides, water vapour transport, and for contaminant remediation (Amali *et al.*, 1994; Chen *et al.*, 2000; Arthur *et al.*, 2014b). Until recently, the hysteresis of soil water vapour sorption isotherms, where adsorption processes dominate (Tuller *et al.*, 1999; Tuller & Or, 2005a), was assumed to be negligible. For example, Rose (1971) noted that although hysteresis in dry soils may be real and complicated, its effect will be masked by environmental factors such as temperature and can, therefore, be ignored. However, several studies have clearly shown that even under very dry conditions hysteresis occurs in both source clays and soil samples (Johansen & Dunning, 1957; Prunty & Bell, 2007; Shvarov & Koreneva, 2008; Arthur *et al.*, 2013; Lu & Khorshidi, 2015). Consideration of hysteresis under such dry conditions is crucial for accurate modelling of water vapour flow in arid regions (Bittelli *et al.*, 2008), for quantification of soil evaporation (Or *et al.*, 2013) and for ensuring correct estimation of soil properties from hygroscopic water content

measurements (Wuddivira *et al.*, 2012). For example, estimation of clay content from desorption water content based on models developed from adsorption data led to errors as large as 12.3% for fine-textured soil samples (Arthur *et al.*, 2015).

There have been a few attempts to quantify water sorption hysteresis for both soil samples and source clay minerals. For example, film flow hysteresis was included when Revil and Lu (2013) developed a unified CEC-normalized water vapour sorption isotherm model for porous clayey materials. Also, we previously suggested a single parameter non-singularity model to account for sorption hysteresis in 21 Arizona soils (Arthur *et al.*, 2013). Further, Lu and Khorshidi (2015), using source clays and silt soil samples, proposed an approach to quantify sorption hysteresis at a given humidity level and also for the full sorption-desorption isotherm. For source clays, the difference in hysteresis between swelling (e.g. smectite) and non-swelling clay minerals (e.g. kaolinite) was attributed to variations in the occurrence of particle surface hydration and cation hydration. Based on the theory that water molecules form clusters on cations prior to complete surface coverage (Prost *et al.*, 1998; Laird, 1999), studies have confirmed that the cation exchange capacity (CEC) and cation type play a crucial role in water vapour sorption magnitude and hysteresis. For example, Woodruff and Revil (2011) showed for source clay minerals that all the sorption isotherms collapsed into a narrow range for the relative humidity (*RH*) range from 0.05 to 0.70 when the sorbed water contents were normalised by the CEC.

In natural soils (with mixed clay mineralogy and, in some cases, significant amounts of organic carbon) other factors associated with or additive to the two sorption processes (particle surface and cation hydration) may come into play. For example, the width of the hysteresis loop was reported to decrease as the soil specific surface area decreases (Globus & Neusypina, 2006). Further, water sorption isotherms (−1 to −100 MPa) measured for nine samples with an organic matter (OM) content range from 16.1 to 86.1 g kg^{-1} revealed that OM was also positively correlated to the

magnitude of hysteresis in microaggregates (Zhuang *et al.*, 2008). Thus, it is clear that the clay mineralogy, OM content and CEC all play a vital role in water vapour sorption hysteresis, particularly for clay minerals. However, this role has not been clarified properly for natural soils. Hence, the objectives of the study were to: (i) propose an index to quantify sorption hysteresis and evaluate it based on measured water vapour sorption isotherms for source clay minerals and soil samples comprising various amounts of clay and organic carbon, and (ii) identify the role of clay mineralogy, soil texture, organic carbon content and cation exchange capacity on soil water vapour sorption hysteresis.

Methodology

Investigated samples

The samples considered for this study included four source clay minerals and 147 soil samples from 24 countries across five continents (Europe 42, North America 61, South America 15, Africa 25 and Asia 4) (Table S1). The source clay mineral samples included calcium smectite from Mississippi (Ca-S), sodium smectite from Wyoming (Na-S), illite from Illinois (IL) and kaolinite from Georgia (KA). The soil samples were grouped into five classes based on their clay mineralogy, the ratio of CEC to clay content, the shape of the sorption isotherms relative to that of the source clay minerals and soil organic carbon content (SOC) (Table 1). The soil sample groups comprised the following: (i) 27 kaolinitic samples (clay content, CL from 6 to 75 g $100g^{-1}$); (ii) 22 illitic samples (CL from 3 to 72 g $100g^{-1}$); (iii) 58 smectitic samples (CL from 13 to 83 g $100g^{-1}$); (iv) 16 "mixed-clay" samples having approximately equal proportions of kaolinite, illite, and smectite and in some cases chlorite and vermiculite (CL from 2 to 51 g $100g^{-1}$); and (v) 14 SOC-rich samples with illite as the dominant clay mineral (SOC from 2.0 to 8.4 g $100g^{-1}$), denoted as ORG. Further details about the properties of each individual sample are presented in Table S1.

Laboratory measurements

Particle size distribution, organic carbon content, and clay mineralogy

The soil particle size distribution was measured for air-dry samples that were passed through a 2-mm sieve with a combination of wet sieving and the pipette or hydrometer methods after removal of SOC and carbonates (Gee & Or, 2002). Soil organic carbon was measured on milled subsamples via oxidation of carbon at 1800 °C with an elemental analyser coupled to a thermal conductivity detector (Thermo Fisher Scientific, Waltham MA, USA). The SOC of samples containing $CaCO_3$ was computed as the difference between total carbon and inorganic carbon calculated from the percentage of $CaCO_3$. The clay mineralogy was quantified via X-ray diffraction (XRD) with the RockJock software package (Eberl, 2003), which performs a whole-pattern modified Rietveld-type refinement. The CEC of the samples was determined with the ammonium acetate extraction method at pH 7 and at pH 8.2 for 25 samples with high amounts of $CaCO_3$ (Sumner & Miller, 1996).

Water vapour sorption isotherms

All the samples were air dried at stable *RH* conditions of 0.45 prior to the start of measurements. Water vapour adsorption and desorption isotherms covering the range $0.03 \leq RH \leq 0.93$ with a resolution of 0.02 *RH* were measured in duplicate for all considered samples at 25 °C with a vapour sorption analyser (METER Group Inc., Pullman, WA, USA). Because the duplicate measurements were identical, only the second replicate is reported here. Full details of the methodology are provided by Arthur *et al.* (2014a). After completion of measurements, the samples were oven dried for 48 hours at 105 °C to determine the reference water content.

Quantification of hysteresis

Hysteresis of the sorption isotherms was quantified by estimating the hysteresis at a given point and then using that estimate to compute the average hysteresis over a prescribed *RH* range. First, the

local hysteresis at a specific *RH* value (H_s) was estimated as the difference between the water content retained after desorption (w_d) from that obtained from adsorption (w_a) at a given point *i* (Equation 1) (Zhuang *et al.*, 2008).

$$H_s = (w_d - w_a) \times 100 \quad (1)$$

Second, the average hysteresis (H_A) over a prescribed *RH* range was determined by computing H_s for a selected *RH* range (*x* and *y*) and dividing by the number of selected data points (*n*) (Equation 2). Although the sorption isotherms were measured for the range $0.03 \leq RH \leq 0.93$, for the estimation of H_A, only the range $0.1 \leq RH \leq 0.8$ was used for estimation of H_A in order to omit the regions where the isotherms converge. The selected *RH* range yielded approximately 36 data points ($n = 36$) for each sample.

$$H_A = \left[\left(\sum_{i=y}^{i=x} w_d - w_a \right) / n \right] \times 100 \quad (2)$$

A conceptual presentation of the hysteresis quantification approach is shown in Figure 1. To evaluate the suitability of Equations (1) and (2) to accurately characterize the H_s and H_A, of water vapour sorption isotherms, we evaluated two scenarios. For scenario 1, we selected the water vapour sorption isotherms of a soil sample dominated by Ca-S and composed of 69, 30, 1, and 0.1 g $100g^{-1}$ of clay, silt, sand, and SOC, respectively. For every measured data point, an empirical value of 0.03 g g^{-1} of water was added to the measured isotherm to generate a similar-shaped isotherm (identical hysteresis), but shifted to larger water contents. This enables to evaluate if the proposed index returns the same values for two samples with similar hysteresis magnitude, but different water contents. For scenario 2, we selected the sorption isotherm of the Na-S clay mineral and generated a second isotherm where the adsorption water content was kept constant and the desorption water

content was increased by an average of 20%. Scenario 2 evaluates if the indices reflect the differences in hysteresis magnitude for the two isotherms.

Statistical Analyses

To evaluate the effect of clay mineralogy, clay and SOC contents and CEC on H_A, we first assessed the normality (Shapiro-Wilk test) and constant variance (computing the Spearman rank correlation between the absolute values of the residuals and the observed values of H_A) of the data. Thereafter, a linear regression was conducted for the soil properties (except clay mineralogy) and the H_A for the soil samples from the four clay mineral groups (KA, IL, SM, and MX).

The effect of clay mineralogy on H_A was examined via one-way analysis of covariance with the dominant clay mineral as the *factor* and clay content and SOC as the *co-variates*. For each sample group, the H_A values were adjusted to an average clay content (38 g $100g^{-1}$) and SOC content (1.03 g $100g^{-1}$) for the entire dataset. The Holm-Sidak posthoc test was used to differentiate the means of the different groups at the significance level of 0.05. This was because the samples within the various groups had different ranges in clay content (mean clay content values were 37, 23, 50, and 24 g $100g^{-1}$ for the KA, IL, SM and MX groups, respectively).

Results and discussion

Water vapour sorption hysteresis and evaluation of hysteresis index

An example of a typical water vapour sorption isotherm loop is depicted in Figure 1. Hysteresis was present in all the source clays (except the kaolinite clay mineral) and soil samples, albeit at different magnitudes. The occurrence of hysteresis in soil water sorption isotherms has been observed repeatedly within the last decade for different soil textures and matric potential (ψ) range $-0.5 \leq \psi \leq -50$ MPa (Prunty & Bell, 2007; Zhuang *et al.*, 2008). Sorption hysteresis is also documented for both source clays and different types of soil in the range $0.03 \leq RH \leq 0.95$ ($-483 \leq \psi \leq -10$ MPa) (Shvarov & Koreneva, 2008; Arthur *et al.*, 2013; Lu & Khorshidi, 2015).

The prevalence of hysteresis has led to the development of several approaches to quantify hysteresis. The approaches include computing the difference between adsorption and desorption at a given *RH* similar to Equation (1) (Zhuang *et al.*, 2008), scaling that difference by the average water content (Lu & Khorshidi, 2015), or by fitting theoretical models to the isotherm data and using the parameters to estimate hysteresis (Arthur *et al.*, 2016). To evaluate the effect of soil properties on water vapour sorption hysteresis, it is important to employ a consistent approach. Results of the evaluation of Equations (1) and (2) for accurate quantification of hysteresis are presented in Figure 2. For scenario 1 (Figures 2ab), the two isotherms presented in Figure 2a exhibited identical values of the maximum H_s of 1.7% at the same *RH* of 0.22 (Figure 2b). The shape of the isotherms was also similar to the H_s trend; for $RH>0.22$, H_s decreased until $RH\sim0.42$ followed by an increase until $RH\sim0.78$. Further, both isotherms had H_A values of 1.49% for the considered *RH* range from 0.1 to 0.8. This suggests that the proposed hysteresis index is unaffected by the magnitude of water content and accurately reflects the trends in local and average hysteresis. For scenario 2 (Figures 2cd), the two different isotherms (one with larger desorption water content) exhibited different levels of H_s for a given *RH*, although the *RH* at which H_s was maximum was identical (0.58) for the

two samples. The estimated H_A values for the two isotherms were 4.28 and 6.13%, respectively, for the original measured isotherm and the generated more hysteretic isotherm. Thus, it is also clear that H_A is able to identify differences in hysteresis between the two samples in Figure 2c, regardless of the isotherm shape. Consequently, the two indices were utilized in the subsequent discussions about factors contributing to the occurrence of hysteresis in the clay minerals and soil samples.

Hysteresis of source clay minerals

Sorption isotherms and the estimates of hysteresis for the range $0.1 \leq RH \leq 0.8$ for the four clay minerals (KA, IL, Ca-S, and Na-S) are presented in Figure 3. The insets depict the local hysteresis within the selected *RH* range. Among the four minerals, Ca-S had the largest water content at any given *RH*, whereas the KA had the smallest water content – a consequence of the differences in specific surface areas measured with the ethylene glycol monoethyl ether method (SA_{EGME}). The SA_{EGME} values were 811 and 88 $m^2\ g^{-1}$for Ca-S and KA, respectively. The Na-S and IL, respectively, had SA_{EGME} of 279 and 139 $m^2\ g^{-1}$. In addition to differences in sorbed or desorbed water contents, the clay minerals exhibited markedly different isotherm shapes and magnitudes of hysteresis. The two smectite minerals (Ca-S and Na-S) and the IL exhibited significant hysteresis but the KA was largely non-hysteretic. The general mechanisms underlying the smaller water contents sorbed during adsorption compared to desorption were put forward by Lu and Khorshidi (2015) for both swelling and non-swelling clays. The two mechanisms proposed were particle surface hydration and interlayer cation hydration. For non-swelling minerals (e.g. KA, Figure 3a), sorption/desorption is governed by particle surface hydration. As the mineral surface is exposed to the air-filled space, only the heat of evaporation and liquefaction are relevant for water sorption or desorption. Consequently, the sorption and desorption processes are reversible with all the adsorbed water being desorbed at any given *RH*. This was evident for KA where hysteresis was largely absent, and H_s was close to zero for the *RH* range considered and the average (H_A) was 0.16%. The

absence of, or limited, hysteresis in KA sorption isotherms has been reported elsewhere (Martin, 1959; Likos & Lu, 2001). For the swelling minerals (Ca-S and Na-S; Figure 3cd) and to an extent the IL, both hydration processes were responsible for sorption. Particle surface hydration is reversible and does not likely contribute to hysteresis, whereas interlayer cation hydration is crucial to hysteresis (Lu & Khorshidi, 2015). During adsorption, the small initial water content and interlayer distance, coupled with strong Van der Waals attractive forces presume that uptake of water into the interlayer space is restricted and proceeds one water layer at a time as the plates separate only enough to admit one molecular layer at a time (Mooney *et al.*, 1952). At the end of the adsorption cycle (*RH*~0.93 in this case), all the interlayer cations are surrounded by several molecular layers of water, and the prevailing cation (e.g., Na^+ or Ca^{2+}) determines how tight the water is bound and how wide the clay platelets are separated. The water molecules in the Ca-S clay mineral are bound more tightly than in the Na-S (Kuligiewicz & Derkowski, 2017), and at a given *RH* value, the spacing between the clay platelets for Na-S is smaller than for the Ca-S (Keren & Shainberg, 1975). During desorption, however, the sample already has large water content and interlayer distance, resulting in weak attraction forces; dehydration starts from the surface of the mineral, where all the sorbed water desorbs (Lu & Khorshidi, 2015). In the interlayer space, the now hydrated cations do not release all the previously adsorbed water molecules at a given *RH*. This mechanism is less pronounced in the 2:1 IL clay with H_A of 0.51%, likely due to the smaller surface area of the IL compared to Na-S or Ca-S, and presence of K^+ ions in the interlayer (Figure 3b). The H_s of IL consistently increased with increasing *RH* (Figure 3b inset), thus the maximum H_s occurred at the end of the *RH* range considered (0.80). From Figures 3cd, the incomplete release of the adsorbed water molecules is more prevalent for Na-S than for Ca-S, as confirmed by the larger H_A value obtained for Na-S (4.33%) compared to Ca-S (1.92%). The insets of Figures 3c and 3d show the dynamics of H_s with increasing *RH* for Ca-S and Na-S. The H_s for Ca-S increased until

RH~0.2, followed by a gradual decrease until 0.55 and further increase from 0.6 to 0.80 (Figure 3c). For Na-S, the undulating nature of the desorption isotherms is clearly reflected in the trend of H_s with *RH* (Figures 3d). The undulating nature of the desorption isotherm is because of the weak attractive force between the interlayers that are further apart after adsorption.

Impact of clay and organic carbon contents on sorption hysteresis

This section evaluates the impact of soil clay and SOC contents on the magnitude of hysteresis for the soil samples. The sorption isotherms of two smectitic samples from Texas, both composed of calcium smectite, with different clay content (33 and 55 g $100g^{-1}$) and similar silt (41 and 42 g $100g^{-1}$)and SOC (0.8 g $100g^{-1}$) content are presented in Figure 4a. The sample with 55 g $100g^{-1}$ clay had a higher magnitude of hysteresis (0.93%) than the soil sample with 33 g $100g^{-1}$ clay (0.55%). Similarly, two illite-rich soil samples that had 14% clay but significantly different SOC contents showed considerably different magnitude of hysteresis; the small (2.13 g $100g^{-1}$) and large (8.42 g $100g^{-1}$) SOC soils exhibited H_A values of 0.27% and 0.68%, respectively (Figure 4b). These results suggest that for soil samples that have identical clay mineralogy, hysteresis tends to increase with clay content and SOC.

A scatter diagram containing H_A vales for all 147 soil samples as a function of clay content (Figure 5a) shows that: soil samples dominated by illites, smectites, or mixtures thereof, provided a significant increase ($p<0.001$; $R^2 = 0.92$) in the magnitude of hysteresis with increasing clay content well represented by a single regression; samples dominated by kaolinite with $0.01 \leq H_A \leq 0.69\%$ possess a much weaker correlation with clay content. As H_A does not appear to depend on large water content associated with a high proportion of clay in soil (Figure 2), the mechanism responsible for the increase in hysteresis with clay content is not clear. Globus and Neusypina (2006) identified a few soils where hysteresis was more prominent for those that are fine-textured than for those with coarse-texture. Globus and Neusypina (2006) identified a few soils where

hysteresis was more prominent for those that are fine-textured than for those with coarse-texture. For a given soil sample (clay type, silt and SOC content), as clay content increases the population of surface sites increases uniformly in relation to their energy distribution so the population of the most favourable adsorption sites increases. More water is consequently able to bind strongly to mineral surfaces. The fraction of water molecules able to desorb, at a given *RH*, depends on this population and is decreased which is reflected in an increased degree of hysteresis.

The ORG soil samples tended to have larger H_A values for a given clay content than the rest of the sample groups (Figure 5a). The relationship between H_A as a function of SOC (for the samples with high SOC) shows a high linear dependence (Figure 5b). The size of the data symbols signifies the magnitude of clay content of each of 14 samples and suggests that this content has little influence on H_A in these cases. Zhuang *et al.* (2008) examined hysteresis ($-100 \leq \psi \leq -1$ MPa) for nine samples with a range $1.61 \leq$ SOC $\leq$ to 8.6 g $100g^{-1}$ and also found increased hysteresis with increasing SOC.The increase in the magnitude of hysteresis as SOC increased may be related to conformational changes in the structure of OM during the sorption process. The organic soil matrix has a strong affinity for water molecules, as functional groups such as carboxylic, phenolic hydroxyl and amino groups provide sorption sites for water molecules (Hurraß, 2006). The orientation of these hydrophilic and of hydrophobic functional groups at the surface of soil OM slowly change during sorption-desorption cycles (Mashum & Farmer, 1985; Valat *et al.*, 1991). At low water contents (at the start of the adsorption process) there may be a hydrogen bond-based crosslinking of organic matter segments by water molecules resulting in a more rigid structure (Schaumann & Leboeuf, 2005), and a relatively smaller amount of sorbed water at a given *RH*. During desorption, a slow reorientation of the functional hydrophobic groups occurs and sorption sites that were originally inaccessible at lower *RH* values (due to the previous orientation) are now covered with water molecules. At the same *RH*, the water molecules are not desorbed

correspondingly. The larger the SOC content, the stronger this mechanism becomes and the higher the magnitude of hysteresis.

It is therefore clear that both clay and SOC control water vapour hysteresis to a significant degree (Figure 5ab). A multiple regression of all the soil samples together (excluding the KA samples) showed that H_A can be estimated from a combination of clay and SOC contents (Equation 3).

$$H_A = -0.073 + 0.021 \times \text{clay} + 0.057 \times \text{SOC}$$
$$\text{Adj. } R^2 = 0.92;\ p<0.001 \qquad (3)$$

where H_A, clay and SOC contents are all in %.

Soil clay mineralogy and CEC effect on hysteresis

The significant differences in the magnitude and dynamics of hysteresis between the four (pure) clay minerals (Figure 3) exert their influences in soil together with contributions from other components such as oxides, carbonates and SOC in a wide variety of compositions. This poses a challenge to identify the contribution each component makes to sorption hysteresis. Comparison of H_A values for three soil samples with clay content ~43 g $100g^{-1}$ but predominant in either KA, IL or SM show hysteresis in the order SM>IL>KA (Figure 6a). So, at least, an inkling of the contributions made by the individual clays is discernible. However, the clay fraction in most soils comprises several minerals in various proportions. The sample groups (Table 1) classify such various proportions in clay and SOC contents. The result of one-way analyses of co-variance where clay content and SOC were used as co-variates to isolate the effect of clay mineralogy on the H_A values of the different groups (Figure 6b). Consistent with Figure 3 and Figure 6a, the adjusted mean of the H_A values for the SM samples (0.87%) was about 3 times that of the KA (0.28%) and about 1.3 times larger than the H_A values of the IL and MX (0.64 and 0.67%) samples. This is in agreement with the previous discussion on the different mechanisms (surface hydration, interlayer

cation hydration) in which water sorbs and desorbs on the different clay minerals. The quantitative clay mineralogical data revealed that some of the KA samples had small amounts of IL and SM minerals and this may account for some hysteresis in those samples as KA has a low CEC and no interlayer hydration (Figure 3a). A similar observation was made by Lu and Khorshidi (2015) for source clay minerals where as little as 10% Na-S mixed with 90% KA led to a large increase in average hysteresis that was even significantly larger than the Ca-S sample in their study.

The CEC of natural soil samples emanates from clay mineralogy, clay and SOC contents. As discussed above, the three properties have varying effects on water vapour sorption hysteresis. Combining all soil samples, the CEC better explained the trends observed in H_A regardless of the clay mineralogy, clay or SOC contents (Figure 7). This confirms the theory that for samples with elevated CEC, the cation hydration mechanism plays a significant role for the amount of water sorbed as well as the magnitude of hysteresis (Woodruff & Revil, 2011; Lu & Khorshidi, 2015). The strong correlation between CEC and H_A suggests that it will be practical to estimate the magnitude of H_A of a sample if its CEC is known. This can be useful for applications such as (i) inclusion of hysteresis phenomena in vapour sorption models that hitherto ignored it, and (ii) estimation of desorption isotherms from adsorption isotherms or vice versa.

Conclusions

A soil water vapour sorption hysteresis quantification index based on the difference in water content between the adsorption and desorption isotherms was proposed and evaluated with measured sorption isotherms for the relative humidity range $0.1 \leq RH \leq 0.8$ for source clay minerals and soil samples. The index was unaffected by the magnitude of water content and accurately reflected hysteresis dynamics for the considered *RH* range. Hysteresis, based on the proposed index, was markedly dissimilar for the clay minerals due to different sorption mechanisms on the mineral surfaces and in the interlayers. While kaolinite did not exhibit hysteresis, sodium smectite and

calcium smectite showed strong hysteretic behaviour in the considered *RH* range. For soil samples, the average hysteresis resulted from an interaction between the prevailing dominant clay mineralogy, the clay content and the organic carbon content, all of which reflected in the CEC values. In general, hysteresis was larger for samples with smectitic or illitic clay mineralogy than for kaolinitic samples, and for samples with higher clay contents. Soil organic carbon also correlated positively with average hysteresis for soil samples that were similarly textured. The CEC was the only property that can be used as a proxy for the average hysteresis, as the strong relationship between CEC and average hysteresis was independent of soil type, clay or organic carbon contents.

Acknowledgments

This research was financed by VILLUM FONDEN research grant 13162. We especially thank Dr. Cristine Morgan formerly of Texas A&M University, The International Soil Reference and Information Centre (ISRIC) and Professor Dr. Eric Van Ranst of Ghent University for providing soil samples for this research.

Data Availability Statement

The data that support the findings of this study are available from the corresponding author upon reasonable request.

References

Amali, S., Petersen, L.W. & Rolston, D.E. 1994. Modeling multicomponent volatile organic and water-vapor adsorption on soils. *Journal of Hazardous Materials*, **36,** 89-108.

Arthur, E., Tuller, M., Moldrup, P. & de Jonge, L.W. 2014a. Evaluation of a fully automated analyzer for rapid measurement of water vapor sorption isotherms for applications in soil science. *Soil Science Society of America Journal*, **78,** 754-760.

Arthur, E., Tuller, M., Moldrup, P. & de Jonge, L.W. 2014b. Rapid and fully automated measurement of water vapor sorption isotherms: New opportunities for vadose zone research. *Vadose Zone Journal*, **13**.

Arthur, E., Tuller, M., Moldrup, P. & de Jonge, L.W. 2016. Evaluation of theoretical and empirical water vapor sorption isotherm models for soils. *Water Resources Research*, **52,** 190-205.

Arthur, E., Tuller, M., Moldrup, P., Jensen, D.K. & De Jonge, L.W. 2015. Prediction of clay content from water vapour sorption isotherms considering hysteresis and soil organic matter content. *European Journal of Soil Science*, **66,** 206-217.

Arthur, E., Tuller, M., Moldrup, P., Resurreccion, A.C., Meding, M.S., Kawamoto, K., Komatsu, T. & de Jonge, L.W. 2013. Soil specific surface area and non-singularity of soil-water retention at low saturations. *Soil Science Society of America Journal*, **77,** 43-53.

Bittelli, M., Ventura, F., Campbell, G.S., Snyder, R.L., Gallegati, F. & Pisa, P.R. 2008. Coupling of heat, water vapor, and liquid water fluxes to compute evaporation in bare soils. *Journal of Hydrology*, **362,** 191-205.

Chen, D., Rolston, D.E. & Moldrup, P. 2000. Coupling diazinon volatilization and water evaporation in unsaturated soils: I. Water transport. *Soil Science*, **165,** 681-689.

Eberl, D.D. 2003. User guide to RockJock - A program for determining quantitative mineralogy from X-Ray diffraction data. In: *Open-File Report OF 03-78, 56 p.*

Gee, G.W. & Or, D. 2002. Particle-size analysis. In: *Methods of soil analysis. Part 4. SSSA Book Series No. 5* (eds. Dane, J.H. & Topp, G.C.), pp. 255-293. SSSA, Madison, WI.

Globus, A.M. & Neusypina, T.A. 2006. Determination of the water hysteresis and specific surface of soils by electronic microhygrometry and psychrometry. *Eurasian Soil Science*, **39,** 270-277.

Hurraß, J. 2006. *Interactions between soil organic matter and water with special respect to the glass transition behavior*. Technische Universität Berlin. Doctoral Thesis. https://www.depositonce.tu-berlin.de/handle/11303/1633.

Johansen, R.T. & Dunning, H.N. 1957. Water-vapor adsorption on clays. *Clays and Clay Minerals*, **6,** 249-258.

Keren, R. & Shainberg, I. 1975. Water-Vapor Isotherms and Heat of Immersion of Na-Ca-Montmorillonite Systems .1. Homoionic Clay. *Clays and Clay Minerals*, **23,** 193-200.

Kool, J.B. & Parker, J.C. 1987. Development and evaluation of closed-form expressions for hysteretic soil hydraulic-properties. *Water Resources Research*, **23,** 105-114.

Kuligiewicz, A. & Derkowski, A. 2017. Tightly bound water in smectites. *American Mineralogist*, **102,** 1073-1090.

Laird, D.A. 1999. Layer charge influences on the hydration of expandable 2 : 1 phyllosilicates. *Clays and Clay Minerals*, **47,** 630-636.

Likos, W. & Lu, N. 2001. Automated measurement of total suction characteristics in high-suction range: Application to assessment of swelling potential. *Transportation Research Record: Journal of the Transportation Research Board*, **1755,** 119-128.

Lu, N. & Khorshidi, M. 2015. Mechanisms for soil-water retention and hysteresis at high suction range. *Journal of Geotechnical and Geoenvironmental Engineering*, **141,** 04015032.

Martin, R.T. 1959. Water-vapor sorption on kaolinite: Hysteresis. In: *6th National Conference on Clays and Clay Minerals*, pp. 259-278, New York.

Mashum, M. & Farmer, V.C. 1985. Origin and Assessment of water repellency of a sandy south Australian soil. *Australian Journal of Soil Research*, **23,** 623-626.

Mooney, R.W., Keenan, A.G. & Wood, L.A. 1952. Adsorption of water vapor by montmorillonite. 2. Effect of exchangeable ions and lattice swelling as measured by X-ray diffraction. *Journal of the American Chemical Society*, **74,** 1371-1374.

Nakagawa, K., Saito, M. & Berndtsson, R. 2012. On the importance of hysteresis and heterogeneity in the numerical simulation of unsaturated flow. *Hydrological Research Letters*, **6,** 59-64.

Or, D., Lehmann, P., Shahraeeni, E. & Shokri, N. 2013. Advances in Soil Evaporation Physics-A Review. *Vadose Zone Journal*, **12**.

Pedroso, D.M. & Williams, D.J. 2010. A novel approach for modelling soil water characteristic curves with hysteresis. *Computers and Geotechnics*, **37,** 374-380.

Prost, R., Koutit, T., Benchara, A. & Huard, E. 1998. State and location of water adsorbed on clay minerals: Consequences of the hydration and swelling-shrinkage phenomena. *Clays and Clay Minerals*, **46,** 117-131.

Prunty, L. & Bell, J. 2007. Soil water hysteresis at low potential. *Pedosphere*, **17,** 436-444.

Revil, A. & Lu, N. 2013. Unified water isotherms for clayey porous materials. *Water Resources Research*, **49,** 5685-5699.

Rose, D.A. 1971. Water movement in dry soils. 2. Analysis of hysteresis. *Journal of Soil Science*, **22,** 490-&.

Rudiyanto, Sakai, M., van Genuchten, M.T., Alazba, A.A., Setiawan, B.I. & Minasny, B. 2015. A complete soil hydraulic model accounting for capillary and adsorptive water retention, capillary and film conductivity, and hysteresis. *Water Resources Research*, **51,** 8757-8772.

Sadeghi, M., Babaeian, E., Arthur, E., Jones, S.B. & Tuller, M. 2018. Soil physical properties and processes. In: *Handbook of Environmental Engineering* (ed. Kutz, M.), pp. 137-207. Wiley, Hoboken, NJ.

Schaumann, G.E. & Leboeuf, E.J. 2005. Glass transitions in peat: Their relevance and the impact of water. *Environmental Science & Technology*, **39,** 800-806.

Shvarov, A.P. & Koreneva, E.A. 2008. Hysteresis in the capillary-sorption water potential as dependent on the soil water content. *Eurasian Soil Science*, **41,** 1041-1049.

Sumner, M.E. & Miller, W.P. 1996. Cation Exchange Capacity and Exchange Coefficients. In: *Methods of Soil Analysis Part 3—Chemical Methods* (eds. Sparks, D.L., Page, A.L., Helmke, P.A. & Loeppert, R.H.), pp. 1201-1229. Soil Science Society of America, American Society of Agronomy, Madison, WI.

Tuller, M. & Or, D. 2005a. Water films and scaling of soil characteristic curves at low water contents. *Water Resources Research*, **41,** W09403.

Tuller, M. & Or, D. 2005b. Water retention and characteristic curve. In: *Encyclopedia of Soils in the Environment* (ed. Hillel, D.), pp. 278-289. Elsevier Ltd, Oxford, U.K.

Tuller, M., Or, D. & Dudley, L.M. 1999. Adsorption and capillary condensation in porous media: Liquid retention and interfacial configurations in angular pores. *Water Resources Research*, **35,** 1949-1964.

Valat, B., Jouany, C. & Riviere, L.M. 1991. Characterization of the wetting properties of air-dried peats and composts. *Soil Science*, **152,** 100-107.

van Dam, J.C., Wösten, J.H.M. & Nemes, A. 1996. Unsaturated soil water movement in hysteretic and water repellent field soils. *Journal of Hydrology*, **184,** 153-173.

Woodruff, W.F. & Revil, A. 2011. CEC-normalized clay-water sorption isotherm. *Water Resources Research*, **47**.

Wuddivira, M.N., Robinson, D.A., Lebron, I., Bréchet, L., Atwell, M., De Caires, S., Oatham, M., Jones, S.B., Abdu, H., Verma, A.K. & Tuller, M. 2012. Estimation of soil clay content from hygroscopic water content measurements. *Soil Science Society of America Journal*, **76,** 1529-1535.

Zhuang, J., McCarthy, J.F., Perfect, E., Mayer, L.M. & Jastrow, J.D. 2008. Soil water hysteresis in water-stable microaggregates as affected by organic matter. *Soil Science Society of America Journal*, **72,** 212-220.

Zhuang, L., Bezerra Coelho, C.R., Hassanizadeh, S.M. & van Genuchten, M.T. 2017. Analysis of the hysteretic hydraulic properties of unsaturated soil. *Vadose Zone Journal*, **16**.

Figure captions

Figure 1. Quantification of hysteresis (H) for a water sorption-desorption isotherm. w_d and w_a, water content following desorption and adsorption, respectively, for a given relative humidity (RH) value; H_s, local hysteresis at a specific RH; H_A, average hysteresis calculated from RH values from x to y (0.1 to 0.8 in this study); n, number of RH points selected for computation of H_A (36 points were used in this study).

Figure 2. Evaluation of the proposed method to quantify local hysteresis at selected RH values between 0.10 and 0.80 and the calculated average hysteresis. Values given in the legend of (b) and (d), HA, designate the average hysteresis. "+3g" indicates that 3 g water per 100 g sample was added to each measurement point of SM26 to generate the SM26+3g isotherm; "+20%" indicates that the desorption water contents of the Na-S isotherm was increased by approximately 20% at each RH value to generate the Na-S+20% isotherm. Note that in Figure 2b, the two plots overlap with each other.

Figure 3. Water vapour sorption isotherms of four source clay minerals and the associated degree of local hysteresis, H_S, (insets) for the RH range from 0.1 to 0.8. H_A indicates the average hysteresis for the selected RH range.

Figure 4. (a) Comparison of water vapour sorption isotherms and average hysteresis [H_A] for (a) two smectitic soil samples that have 0.8% organic carbon content and various clay content [provided in legend], and (b) two illitic soil samples that have ~14% clay content and various organic carbon contents [provided in legend].

Figure 5. Relationship between the average hysteresis, H_A, and (a) clay content for soil samples differentiated by clay mineralogy and organic carbon content, and (b) soil organic carbon content. The size of the symbols in (b) signify the magnitude of the clay content. KA, IL, SM, and MX denote samples with kaolinitic, illitic, smectitic, and mixed clay mineralogy, respectively, and ORG signifies organic carbon rich soil samples. Regression in (a) excludes the ORG soil samples.

Figure 6. (a) Comparison of water vapour sorption isotherms for three texturally similar soil samples that are dominated by kaolinite, illite and smectite clay minerals, and (b) Mean average hysteresis corrected for clay and SOC contents for the four soil sample groups. KA, IL, SM, and MX denote samples with kaolinitic, illitic, smectitic, and mixed clay mineralogy, respectively. Letters on bars denote significant differences between the soil sample groups ($p<0.05$).

Figure 7. Relationship between the average hysteresis and cation exchange capacity for soil samples differentiated by dominant clay mineralogy and organic carbon content. KA, IL, SM, and MX denote samples with kaolinitic, illitic, smectitic, and mixed clay mineralogy, respectively, and ORG signifies organic carbon rich soil samples.

Tables

Table 1. Summary of soil textures, organic carbon contents, and cation exchange capacities for the soil groups differentiated by clay mineralogy and soil organic carbon contents. Values denote mean (minimum to maximum); Group ID and number of samples in each group are provided in brackets after sample group name.

Sample Group	Clay (> 2μm)	Silt (2-50μm)	Sand (50-2000μm)	Organic carbon	CEC	Av. CEC/Clay
			/ g $100g^{-1}$		$cmol_{(+)}\ kg^{-1}$	
Kaolinite (KA, 27)	37 (6–75)	23 (8–76)	40 (2–74)	1.07 (0.03–2.93)	8 (3–19)	0.33
Illite (IL, 27)	23 (3–72)	21 (7–41)	56 (6–90)	1.15 (0.10–2.80)	14 (5–26)	0.79
Smectite (SM, 58)	50 (13–83)	33 (9–68)	17 (0–62)	0.97 (0.06–4.32)	47 (11–83)	1.00
Mixed-clay (MX, 21)	24 (2–51)	33 (7–73)	43 (4–91)	1.04 (0.10–3.10)	17 (2–34)	0.77
Organic-rich (ORG, 14)	9 (3–15)	32 (13–61)	59 (30–84)	4.46 (2.00–8.40)	15 (6–29)	1.95

Figures

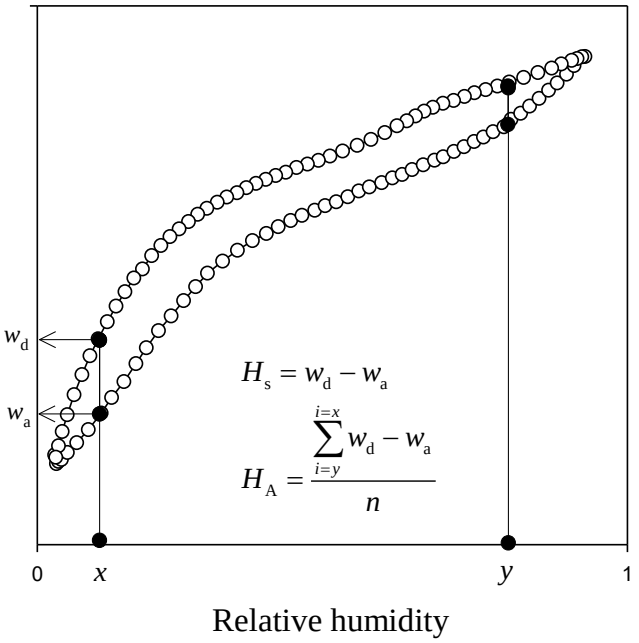

Figure 1. Quantification of hysteresis (H) for a water sorption-desorption isotherm. w_d and w_a, water content following desorption and adsorption, respectively, for a given relative humidity (RH) value; H_s, local hysteresis at a specific RH; H_A, average hysteresis calculated from RH values from x to y (0.1 to 0.8 in this study); n, number of RH points selected for computation of H_A (36 points were used in this study).

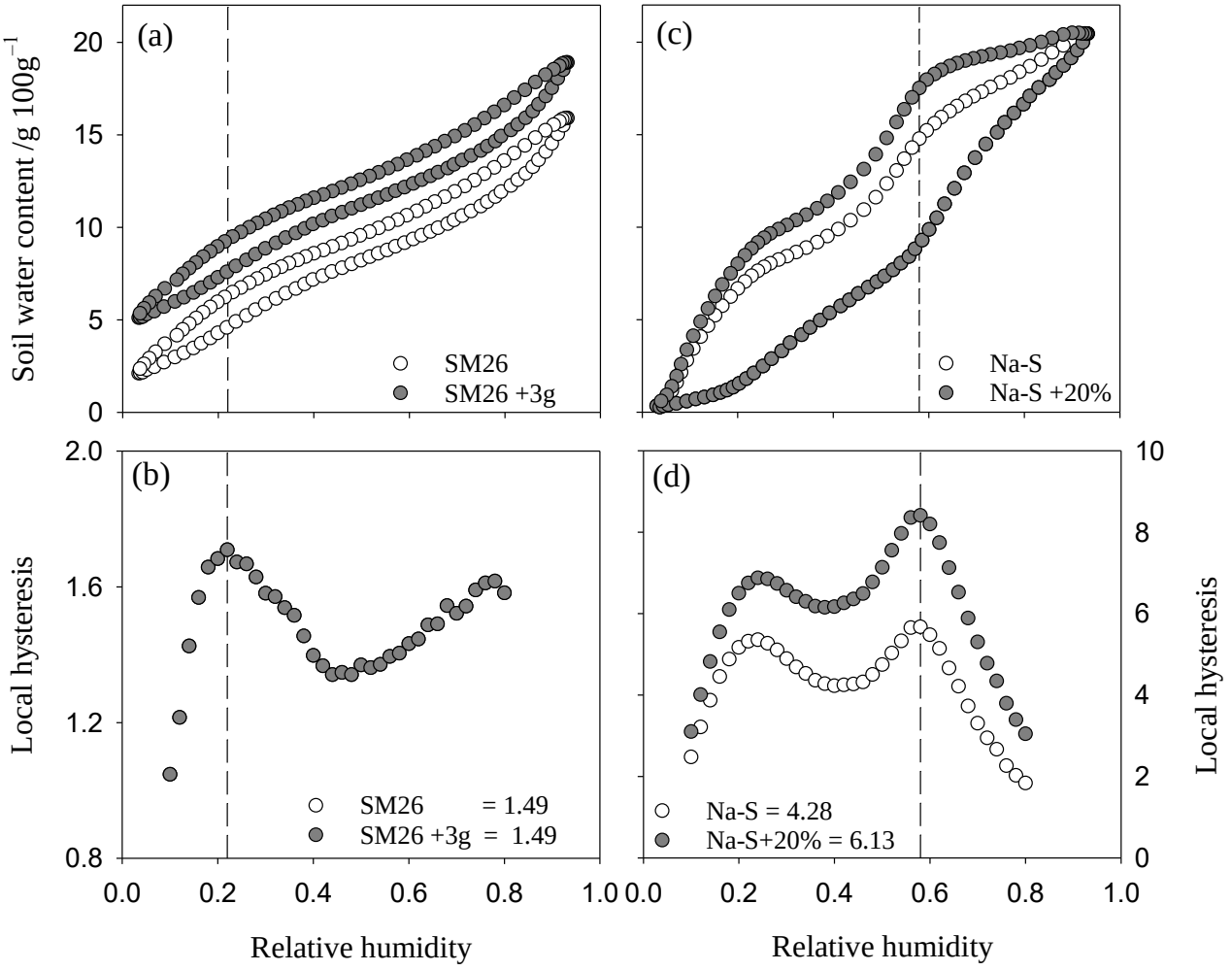

Figure 2. Evaluation of the proposed method to quantify local hysteresis at selected *RH* values between 0.10 and 0.80 and the calculated average hysteresis. Values given in the legend of (b) and (d) designate the average hysteresis. "+3g" indicates that 3 g water per 100 g sample was added to each measurement point of SM26 to generate the SM26+3g isotherm; "+20%" indicates that the desorption water contents of the Na-S isotherm was increased by approximately 20% at each *RH* value to generate the Na-S+20% isotherm. Note that in Figure 2b, the two plots overlap with each other.

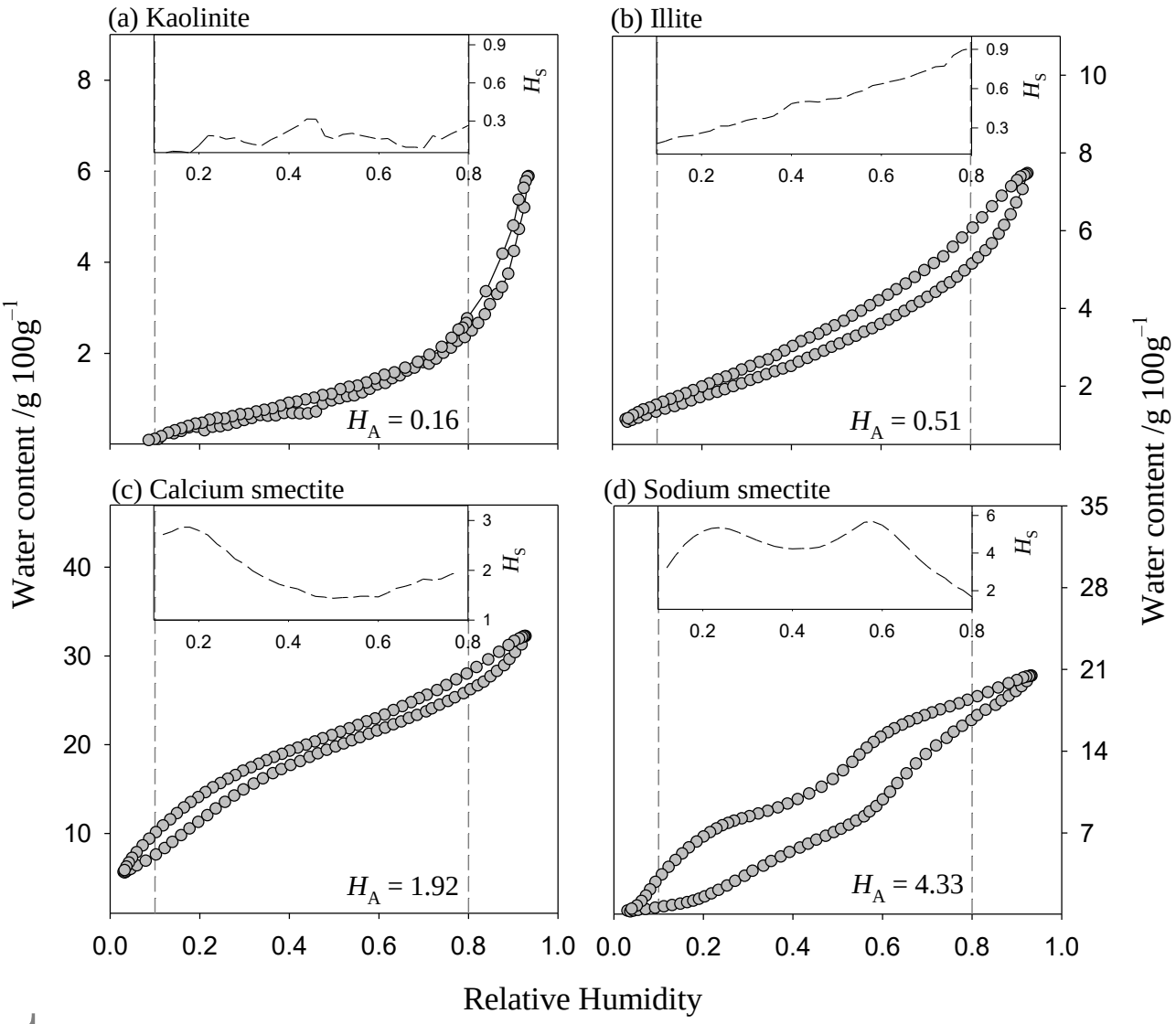

Figure 3. Water vapour sorption isotherms of four source clay minerals and the associated degree of local hysteresis, H_S, (insets) for the *RH* range from 0.1 to 0.8. H_A indicates the average hysteresis for the selected *RH* range.

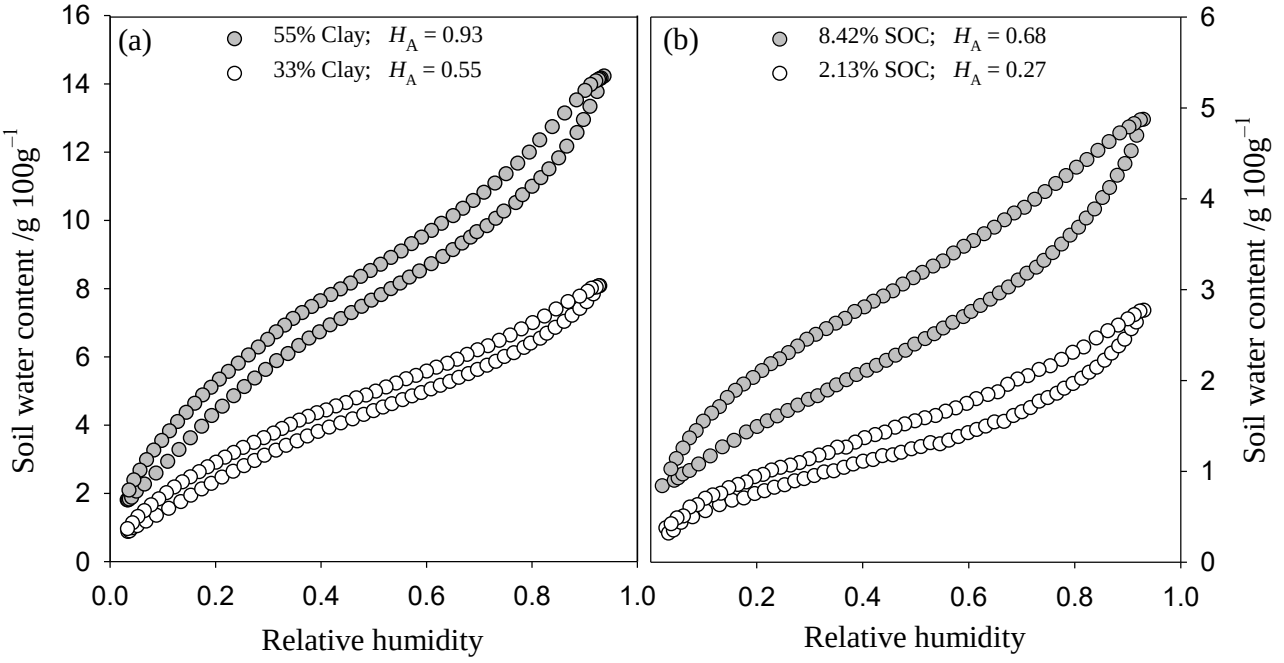

Figure 4. (a) Comparison of water vapour sorption isotherms and average hysteresis [H_A] for (a) two smectitic soil samples that have 0.8% organic carbon content and different clay content [provided in legend], and (b) two illitic soil samples that have ~14% clay content and different organic carbon contents [provided in legend].

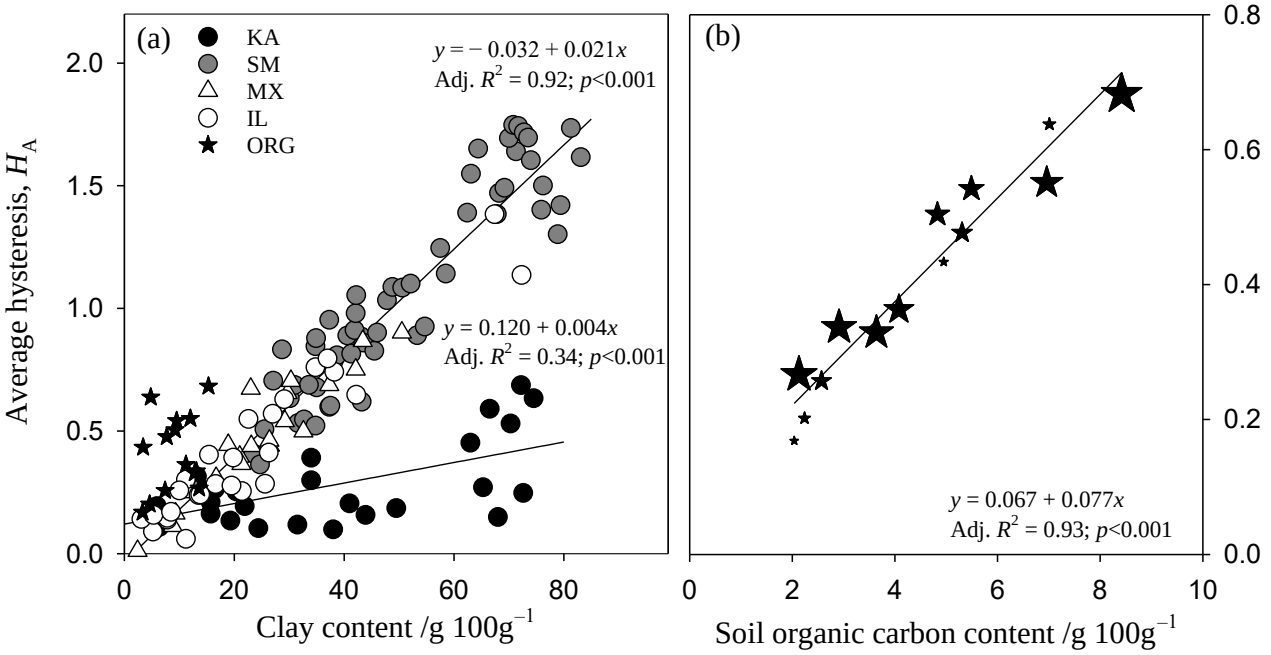

Figure 5. Relationship between the average hysteresis, H_A, and (a) clay content for soil samples differentiated by clay mineralogy and organic carbon content, and (b) soil organic carbon content. The size of the symbols in (b) signify the magnitude of the clay content. KA, IL, SM, and MX denote samples with kaolinitic, illitic, smectitic, and mixed clay mineralogy, respectively, and ORG signifies organic (carbon-rich) soil samples. Regression in (a) excludes the ORG soil samples.

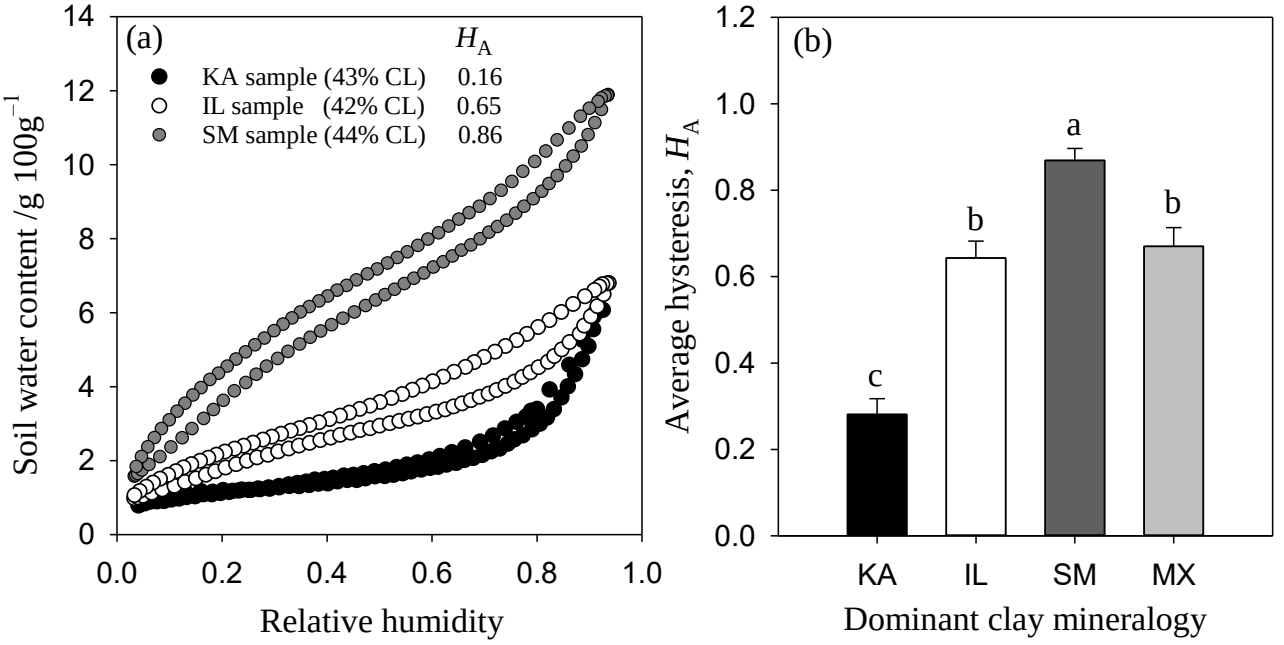

Figure 6. (a) Comparison of water vapour sorption isotherms for three texturally similar soil samples that are dominated by kaolinite, illite and smectite clay minerals, and (b) Mean average hysteresis corrected for clay content and SOC contents for the four soil sample groups. KA, IL, SM, and MX denote samples with kaolinitic, illitic, smectitic, and mixed clay mineralogy, respectively. Letters on bars denote significant differences between the soil sample groups ($p<0.05$).

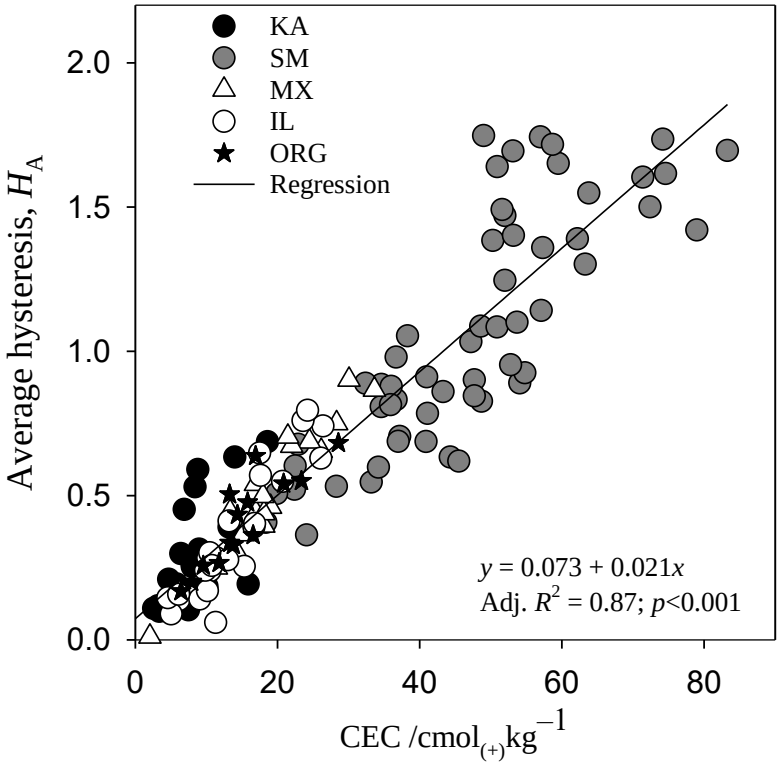

Figure 7. Relationship between the average hysteresis and cation exchange capacity for soil samples differentiated by dominant clay mineralogy and organic carbon content. KA, IL, SM, and MX denote samples with kaolinitic, illitic, smectitic, and mixed clay mineralogy, respectively, and ORG signifies organic (carbon-rich) soil samples.